Supplementary Material: On the demise of Whistler, Horstman and Blackcomb Glaciers, southwest British Columbia, Canada: historical use, recent change and future prospects within a mountain resort

Chloé MONTY[1], Gwenn E. FLOWERS[1], Jeffrey W. CROMPTON[2], Brian MENOUNOS[2,3,4], Caleb MATHIAS[3]

[1]*Department of Earth Sciences, Simon Fraser University, Burnaby, British Columbia, Canada*

[2]*Natural Resources Canada, Geological Survey of Canada – Pacific, Vancouver, British Columbia, Canada*

[3]*Department of Geography, Earth, and Environmental Science, University of Northern British Columbia, Prince George, British Columbia, Canada*

[4] *Hakai Institute, Campbell River, British Columbia, Canada*

Correspondence: Chloé Monty <chloe_monty@sfu.ca>

Remote sensing imagery details

We used high-resolution aerial photographs from the Government of British Columbia from 1973, 1989, 1990 and 2005 to delineate glacier extent (Government of British Columbia, 2025). These images were photogrammetrically processed using Agisoft Metashape (version 2.1.0; https://www.agisoftmetashape.com, last access 17 June 2025) to generate orthoimagery with ground sampling distance (GSD) between 0.11–0.19 m. We also mapped glacier extent from a 2006 aerial orthophoto from the Resort Municipality of Whistler (0.4 m GSD). (Resort Municipality of Whistler, 2006). We mapped glacier extents from spaceborne imagery from three sources of optical satellite imagery, including a 2014 image from Maxar Technologies obtained through Google Earth. This image was captured by the WorldView-3 optical satellite at a resolution of 30 cm (Maxar Technologies, 2025). A 2015 image with 10 m resolution captured by the European Space Agency's Sentinel-2 satellite was also used (ESA, 2025), as were 2016 to 2024 images with 3 m resolution from Planet Lab's PlanetScope satellite constellation (Planet Developers, 2025). The PlanetScope satellites used here were the Dove Classic for 2016–20 and the SuperDove for 2021–24. See

Table S1 for the dates of each image used, their resolution and source.

Glacier extent

See Table S2 for glacier area values and associated errors for Whistler, Horstman and Blackcomb Glaciers, including the western section of Whistler Glacier. See Fig. S1 and S2 for all glacier outlines between 1973–2024. See Fig. S5 for unweighted and piecewise linear regressions (2010/11) for glacier area change.

Climate datasets

The climate datasets used in this study include downscaled CMIP6 air-temperature data (Coupled Model Intercomparison Project, Phase 6) from the Pacific Impacts Climate Consortium (PCIC, 2023), temperature and snowfall measurements from Environment and Climate Change Canada (ECCC) stations (PCIC, 2025), snowfall measurements provided by the avalanche forecasters at Whistler Mountain (2025), and snowfall density measurements from Barton (2017). ERA5-Land geopotential heights (Muñoz Sabater, 2019) were used to assign an elevation to each downscaled CMIP6 gridcell in order to adjust the temperature and accumulation data to the mean elevation of each glacier.

The downscaled CMIP6 data can be accessed from PCIC at https://www.pacificclimate.org/data/statistically-downscaled-climate-scenarios, and the BC weather station data can be accessed at https://www.pacificclimate.org/data/bc station-data. The ERA5-Land data can be accessed at https://cds.climate.copernicus.eu/datasets/reanalysis-era5-land?tab=overview.

Temperature lapse rate

See Fig. S7 for a map of the weather stations used to calculate the temperature lapse rate, and Fig. S8 for monthly temperature lapse rates calculated between April and October 2005–21. The temperature data were binned monthly at each station, and the mean monthly temperatures were used to calculate the temperature lapse rate for months where at least two stations had temperature data available.

Accumulation lapse rate

See Fig. S7 for a map of the weather stations used to calculate the accumulation lapse rate, and Fig. S9 for seasonal (November to April) accumulation lapse rates calculated between 1984–90. All five weather stations used had winter snowfall measurements available from 1983/84 to 1989/90, so the accumulation lapse rate was calculated for each season across the five weather stations.

DDF calculations

See Table S3 for mean elevation and elevation change between LiDAR surveys (27 September 2017, 28 September 2020, 16 September 2024), net balance, accumulation adjusted with an empirical lapse rate, ablation, number of days with positive temperatures between LiDAR survey dates, PDDs and DDFs for Whistler, Horstman and Blackcomb Glaciers.

Disappearance dates for all methods

See Table S4 for projected disappearance dates of Whistler, Horstman and Blackcomb Glaciers using different least-squares linear regressions. See Table S5 for disappearance dates of Whistler, Horstman and Blackcomb Glaciers for different ice-thickness models (Farinotti and others (2019) and Millan and others (2022)), initialisation dates and CMIP6 SSPs. Note that the range of dates reported represents the range calculated for DDFs using ice densities of 790 to 910 $\mathrm{kg\,m^{-3}}$.

Spatially distributed projections of glacier change

See Fig. S10 for spatially distributed glacier loss projected with the mass-balance model for both Farinotti and others (2019) and Millan and others (2022) ice-thicknes models initialized in 2000 under CMIP6 SSP2 with an ice density of 850 $\mathrm{kg\,m^{-3}}$.

Sensitivity of mass-balance model

See Table S6 for the average DDFs and disappearance dates for cases where the density of snow, annual accumulation, and temperature and accumulation lapse rates are varied by $\pm 20\%$ from their reference values and the model is initialised with the Millan and others (2022) ice-thickness distribution in 2007 under CMIP6 SSP2. See Fig. S11 for the associated normalised volume curves.

Rate of area change comparison for Methods 1 and 2

See Table S7 for rates of area change calculated from glacier extent measurements (Method 1) and application of the mass-balance model (Method 2). See Fig. S12 for a comparison of linear regressions from

Method 1 (unweighted, weighted) and Method 2 applied to both the Farinotti and others (2019) model initialised in 2000 and 2007, and the Millan and others (2022) model initialised in 2000 and 2015.

Table S1. Airborne and satellite imagery used to map glacier extent between 1973–2024 with associated date, image type, resolution and source.

Year	Date	Image type	Resolution	Source
1973	08 Aug	Aerial photograph*	0.17 m	BC Lands Service Forest Survey
1985	Unknown	DEM & optical imagery	30 m	TRIM corrected w/ Landsat (Bevington and Menounos, 2022)
1989	22 Jul	Aerial photograph*	0.11 m	BC Surveys and Resource Mapping
1990	16 Jul	Aerial photograph*	0.16 m	BC Surveys and Resource Mapping
2005	24 Sep	Aerial photograph	0.19 m	Selkirk Remote Sensing Limited
2006	Unknown	Aerial photograph	0.40 m	Resort Municipality of Whistler
2014	09 Sep	Optical imagery	0.30 m	Maxar Technologies: WorldView-3 (accessed via Google Earth)
2015	04 Oct	Optical imagery	10 m	European Space Agency: Sentinel-2
2016	16 Aug	Optical imagery	3 m	Planet Labs: PlanetScope
2017	30 Aug	Optical imagery	3 m	Planet Labs: PlanetScope
2018	28 Aug	Optical imagery	3 m	Planet Labs: PlanetScope
2019	27 Aug	Optical imagery	3 m	Planet Labs: PlanetScope
2020	11 Sep	Optical imagery	3 m	Planet Labs: PlanetScope
2021	15 Aug	Optical imagery	3 m	Planet Labs: PlanetScope
2022	31 Aug	Optical imagery	3 m	Planet Labs: PlanetScope
2023	27 Aug	Optical imagery	3 m	Planet Labs: PlanetScope
2024	04 Sep	Optical imagery	3 m	Planet Labs: PlanetScope

*snow-covered

Table S2. Values of glacier area and associated error for Whistler Glacier (main/eastern and western sections), Horstman and Blackcomb Glaciers. All values in m^2.

Year	Whistler (main/east)	Error	Whistler (west)	Error	Horstman	Error	Blackcomb	Error
1973	224,310	1057	74,922	322	467,433	1127	724,913	1610
1985	148,864	57,450	—	—	359,137	90,870	611,882	156,030
1989	197,802	755	66,815	235	—	—	—	—
1990	—	—	—	—	420,064	1203	675,066	1569
2005	72,732	500	33,744	312	283,549	594	451,345	1500
2006	72,405	762	32,250	419	260,112	1073	434,610	1920
2014	58,132	533	25,157	331	223,803	978	384,245	1875
2015	48,899	19,150	27,593	10,770	249,200	29,570	391,821	50,280
2016	56,652	6663	27,251	4158	227,006	10,953	419,272	14,412
2017	48,930	7605	26,449	4239	220,592	12,102	406,488	15,024
2018	33,762	6333	22,629	3084	187,261	9519	364,965	19,533
2019	29,616	5571	19,961	2499	174,486	10,329	362,059	19,602
2020	22,289	5892	16,657	2199	156,055	8244	355,404	19,701
2021	21,203	3894	15,771	1791	150,173	9126	343,328	18,387
2022	—	—	—	—	146,721	9075	—	—
2023	13,026	2160	11,028	2115	128,623	8088	323,115	17,973
2024	11,687	1974	9401	1860	121,245	7995	306,920	19,263

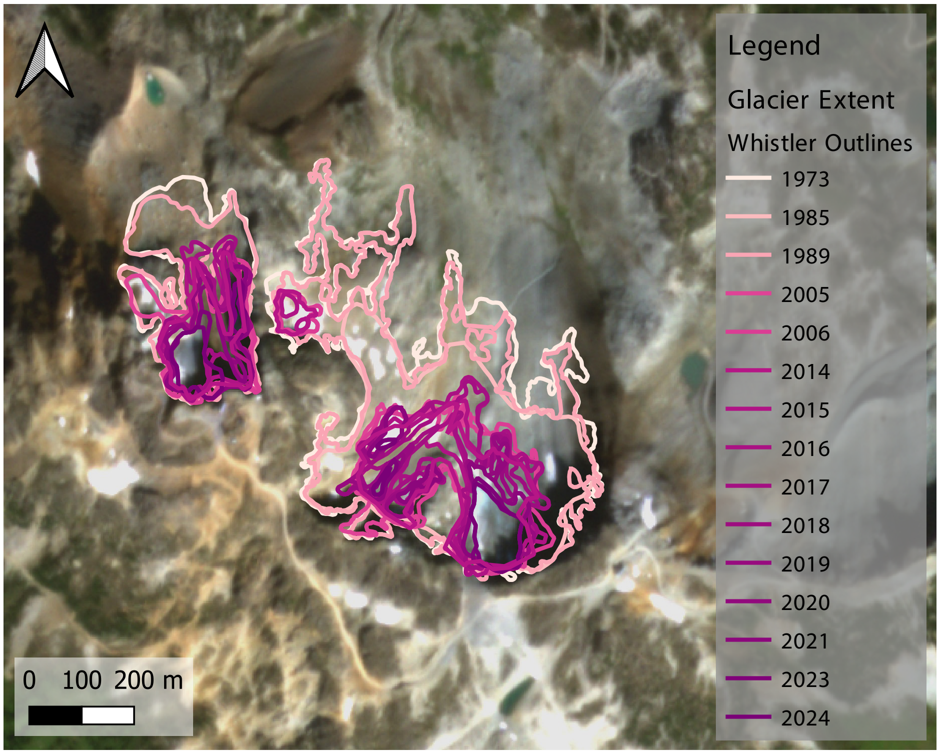

Fig. S1. 1973–2024 Whistler Glacier extents mapped from airborne and satellite imagery. Background image credit: ©2024 Planet Labs PBC.

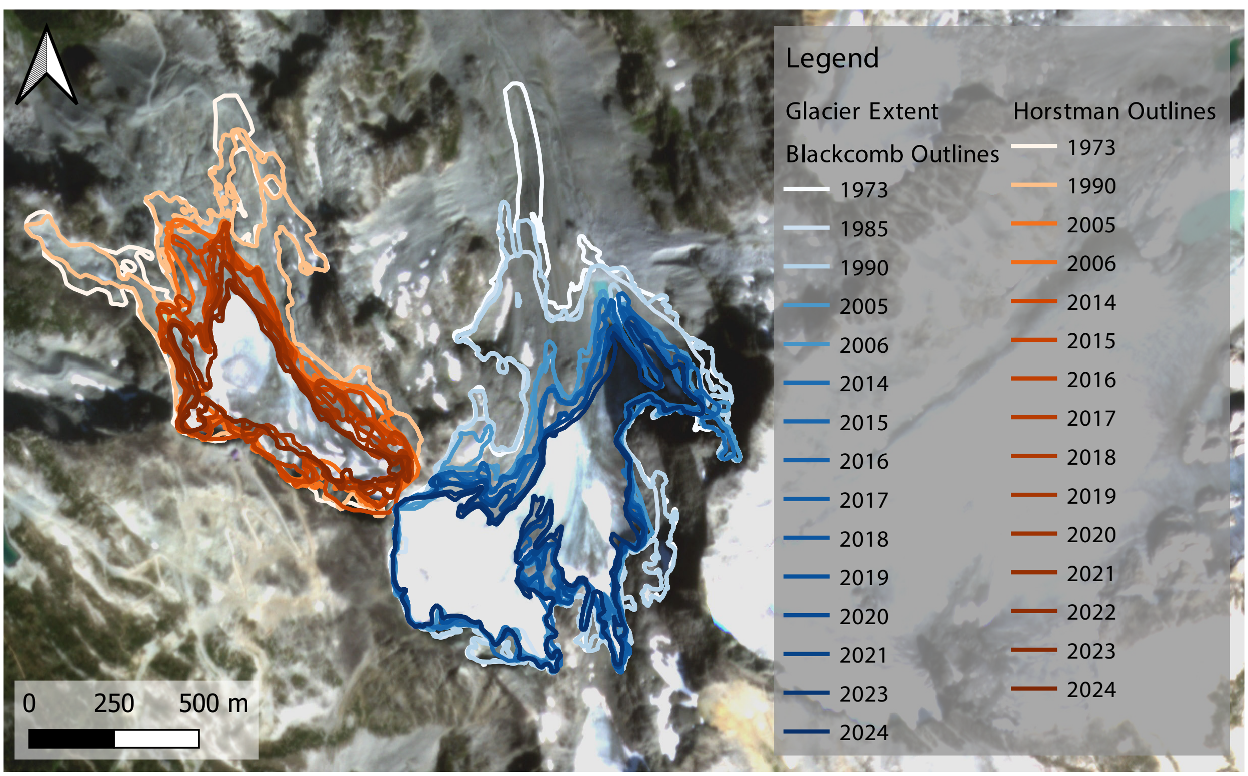

Fig. S2. 1973–2024 Horstman and Blackcomb Glacier extents mapped from airborne and satellite imagery. Background image credit: ©2024 Planet Labs PBC.

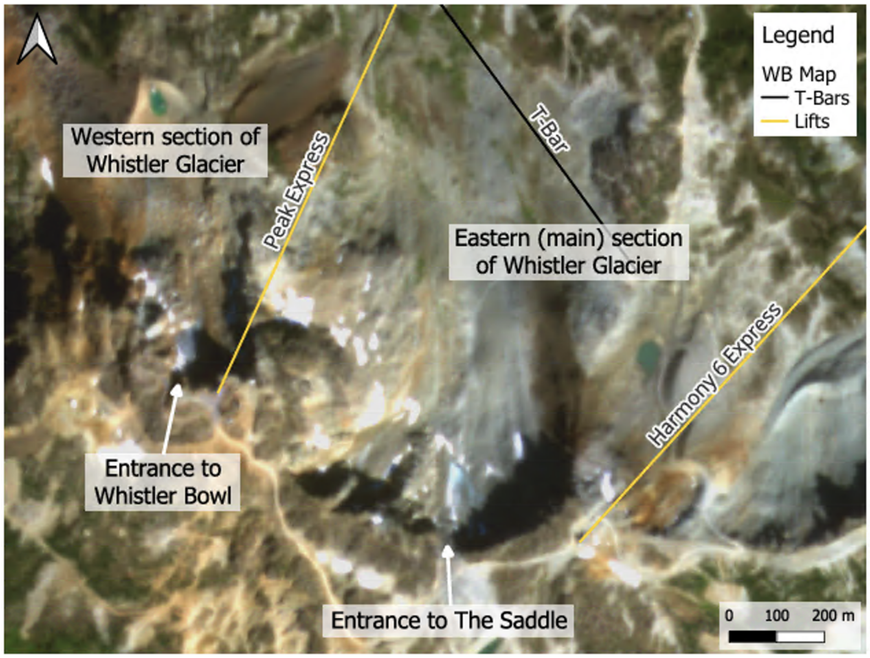

Fig. S3. Map of Whistler Glacier without outlines. Background image credit: ©2024 Planet Labs PBC.

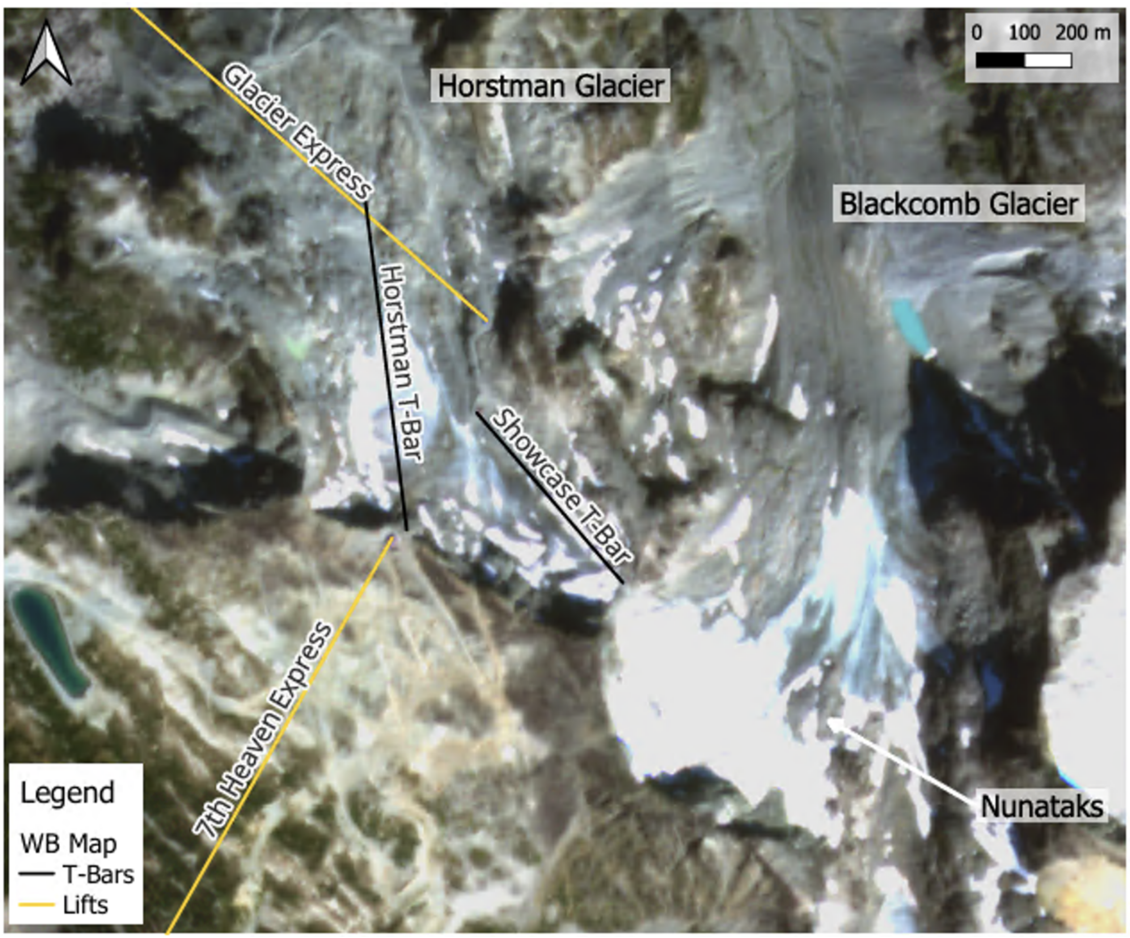

Fig. S4. Map of Horstman and Blackcomb glaciers without outlines. Background image credit: ©2024 Planet Labs PBC.

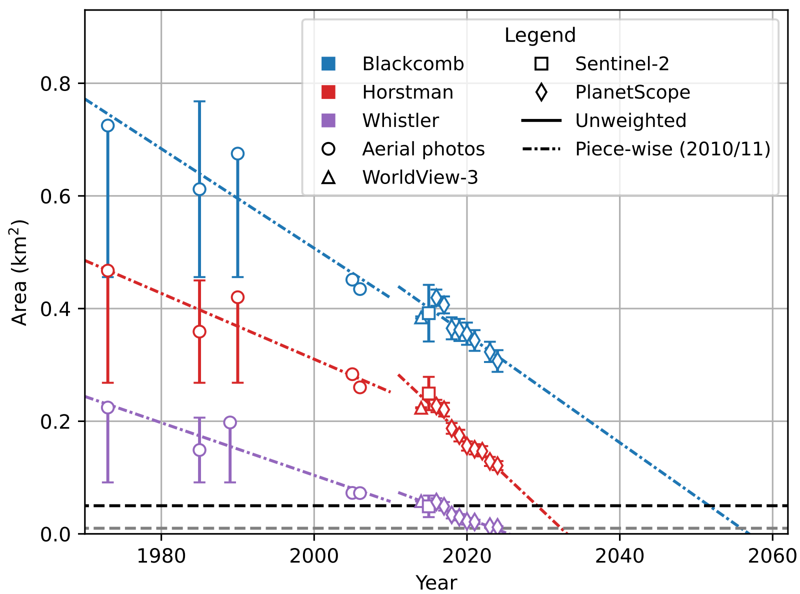

Fig. S5. Timeseries with unweighted and piecewise least-squares linear regressions. ~~Dashed~~ Black dashed line indicates the 0.05 km^2 threshold ~~(Bolch and others, 2010; Leigh and others, 2019; Pelto and Pelto, 2025)~~ (Bolch and others, 2010; Bevington and Menounos, 2022; Pelto and Pelto, 2025) and grey dashed line indicates the 0.01 km^2 threshold (Leigh and others, 2019; Maussion and others, 2023). Piecewise regressions split at 2010/11, calculated using data between 1973–2006 and 2014–24. The regressions post-2011 are all steeper than pre-2010, especially for Horstman Glacier. Note asymmetric uncertainties in 1973, 1989, 1990, where snow cover permitted only an upper bound on area.

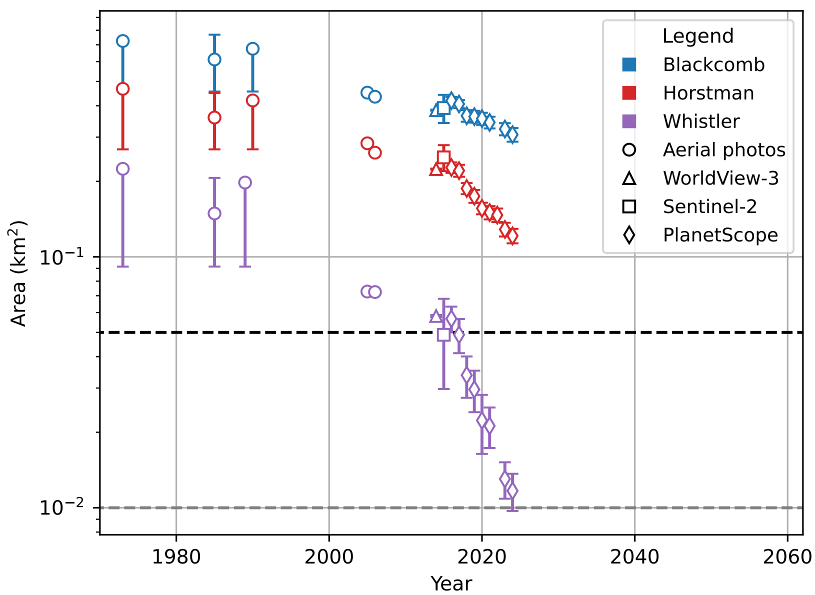

Fig. S6. Semi-log plot with timeseries of glacier extent. ~~Dashed~~ Black dashed line indicates the $0.05\,\mathrm{km}^2$ threshold ~~(Bolch and others, 2010; Leigh and others, 2019; Pelto and Pelto, 2025)~~ (Bolch and others, 2010; Bevington and Menounos, 2022; Pelto and Pelto, 2025) and grey dashed line indicates the $0.01\,\mathrm{km}^2$ threshold (Leigh and others, 2019; Maussion and others, 2023). Note asymmetric uncertainties in 1973, 1989, 1990, where snow cover permitted only an upper bound on area.

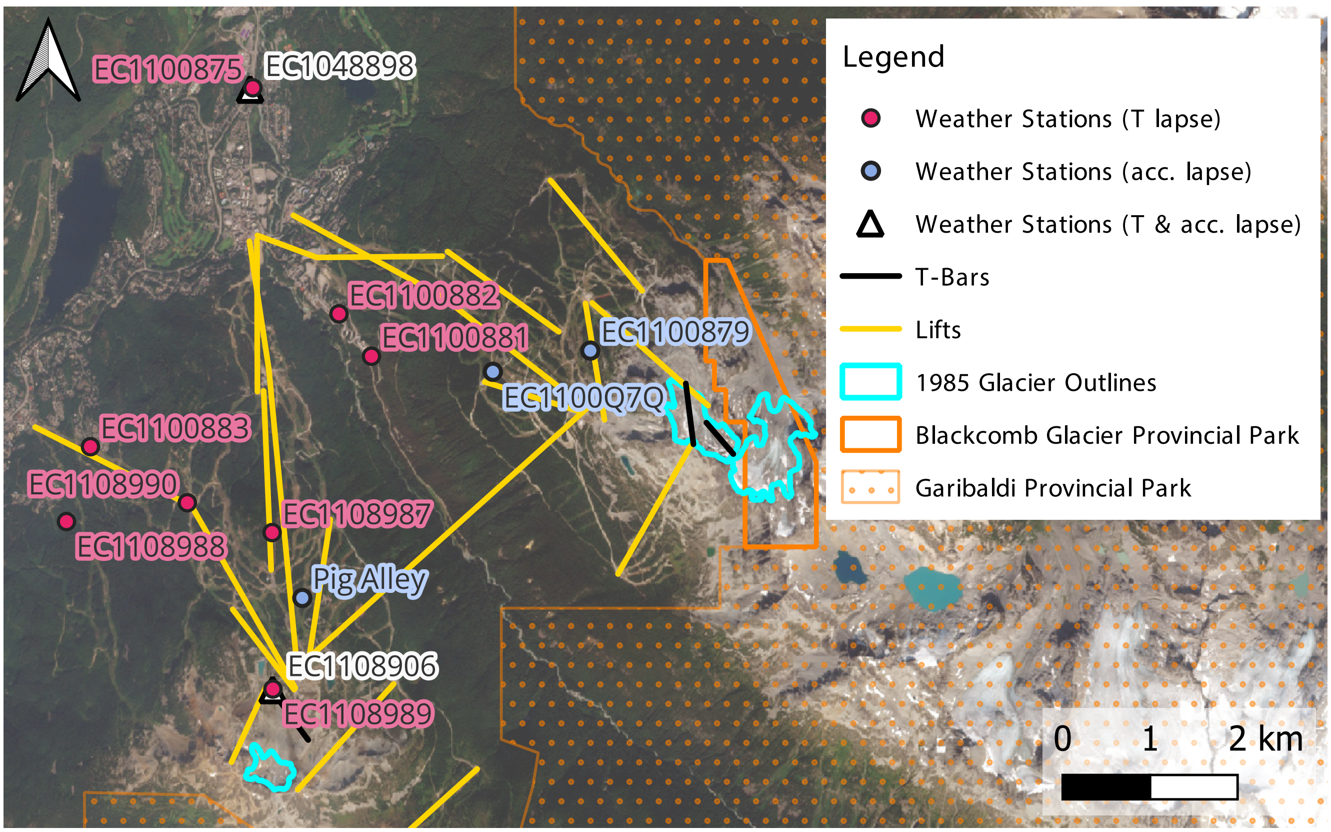

Fig. S7. Overview map showing labelled weather stations. Station names that start with 'EC' represent Environment and Climate Change Canada, data obtained via the Pacific Climate Impacts Consortium (2025). Pig Alley weather station data were obtained from the avalanche forecasters on Whistler Mountain in 2025. Stations shown in magenta were used for temperature (T) lapse rate calculations, stations shown in blue were used for accumulation (acc.) lapse rate calculations, and those represented by white triangles were used for both.

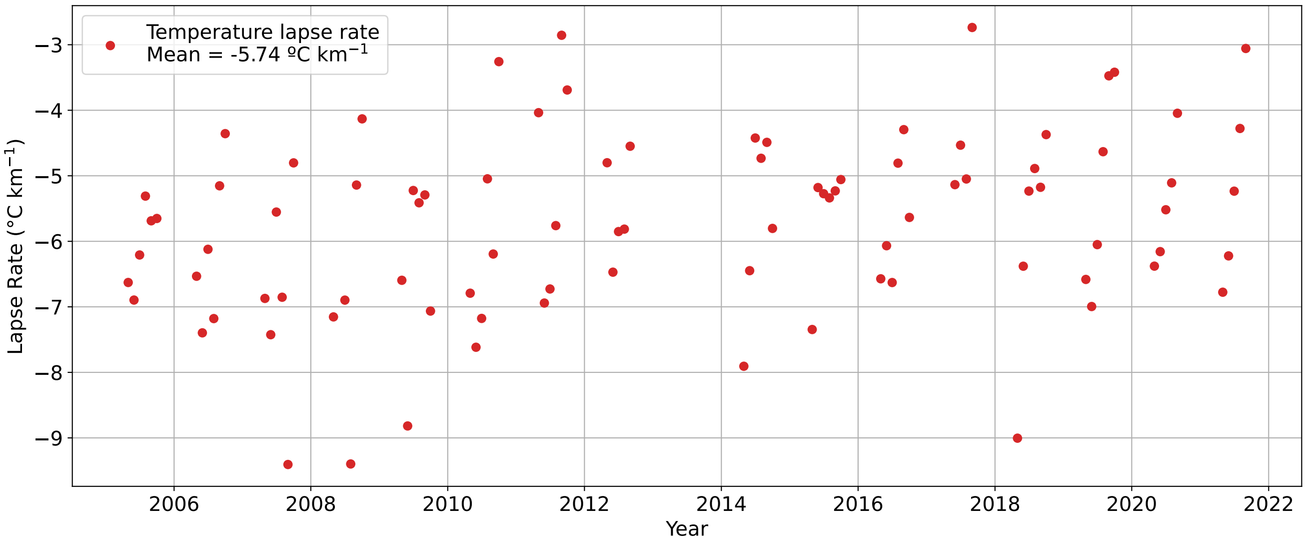

Fig. S8. Monthly temperature lapse rates calculated between April and October 2005–2021. Each point represents a temperature lapse-rate value calculated over a single month where at least two stations had temperature data available.

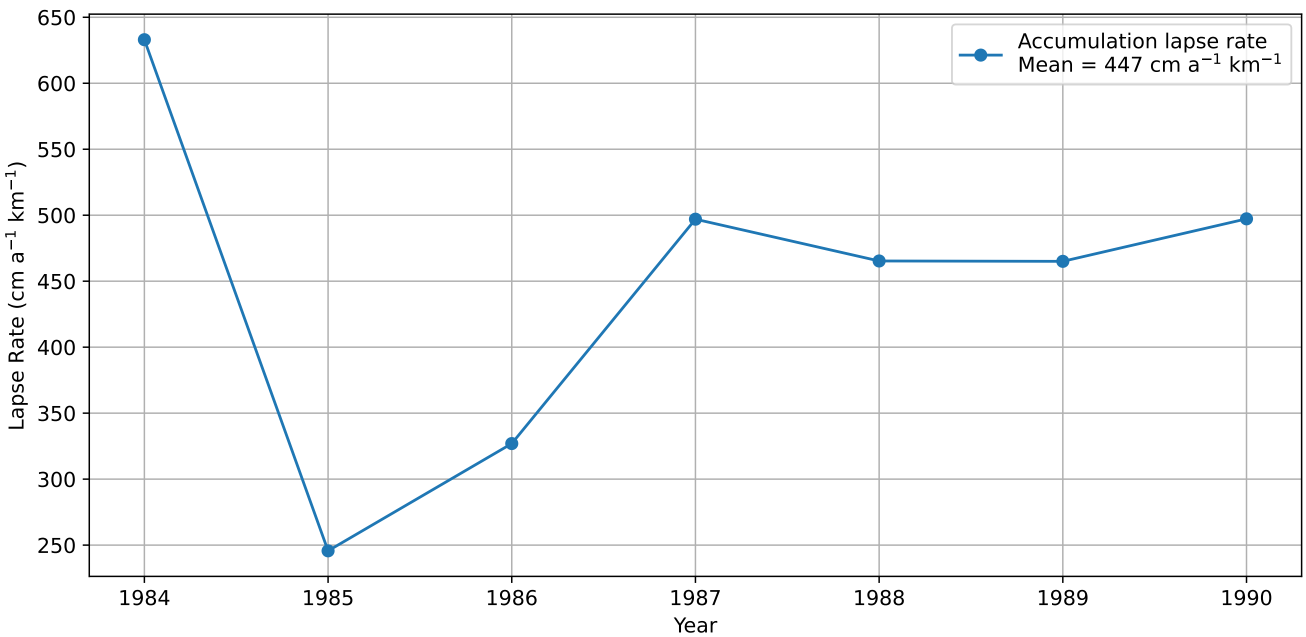

Fig. S9. Seasonal (November to April) accumulation lapse rates calculated between 1984–90. All five stations used had winter snowfall measurements available from 1983/84 to 1989/90.

Table S3. DDF calculation quantities: mean elevation and elevation change between LiDAR surveys (YYYYMMDD: 20170927, 20200928, 20240916), net balance, accumulation adjusted with empirical lape rate, ablation, number of days with positive temperatures between LiDAR survey dates, PDDs and DDFs for Whistler, Horstman and Blackcomb Glaciers.

		Elevation change (m)		Net balance (m w.e.)		Adjusted acc. (m w.e.)		Ablation (m w.e.)	
Glacier	Mean elevation (m)	2017–20	2020–24	2017–20	2020–24	2017–20	2020–24	2017–20	2020–24
Whistler	2006	—	—	—	—	3.18	4.24	—	—
Horstman	2151	-3.16	-5.73	-2.68	-4.86	3.35	4.47	-6.04	-9.34
Blackcomb	2118	-2.50	-5.41	-2.12	-4.59	3.31	4.42	-5.44	-9.01
		# of days		PDD (°C d)		DDF (mm w.e. ° C^{-1} d^{-1})			
		2017–20	2020–24	2017–20	2020–24	2017–20	2020–24	**2017–24 avg**	
Whistler		549	785	4081	5611	—	—	—	
Horstman		519	732	3721	5091	1.50	1.69	**1.60**	
Blackcomb		489	679	3231	4409	1.56	1.89	**1.72**	
							Mean used for Whistler	**1.66**	

Table S4. Disappearance dates of Whistler, Horstman and Blackcomb Glaciers estimated by extrapolating various least-squares linear regressions of glacier area as a function of time: unweighted, weighted inversely proportional to uncertainties (1/err) or the logarithm of uncertainties (1/log(err)), and piecewise (post-2011).

Glacier	Unweighted regression	Weighted (1/err)	Weighted (1/log(err))	Piecewise (post-2011)
Whistler	2027	2035	2027	2026
Horstman	2046	2047	2049	2033
Blackcomb	2063	2070	2065	2057

Table S5. Disappearance dates of Whistler, Horstman and Blackcomb Glaciers for the different ice-thickness models (Farinotti and others (2019) and Millan and others (2022)), initialisation dates (representative of range of acquisition dates of the surface DEMs used by the ice-thickness models) and CMIP6 SSPs. Note that the range of dates for each scenario represents the range calculated for DDFs using ice densities of 790 to 910 $\mathrm{kg\,m^{-3}}$.

Glacier	Ice model	Initialisation date	SSP1	SSP2	SSP5
Whistler	Farinotti	2000	2018–21	2018–21	2018–21
		2007	2023–25	2023–25	2023–25
	Millan	2000	2032–35	2032–35	2032–35
		2015	2042–44	2042–45	2040–42
Horstman	Farinotti	2000	2038–43	2038–43	2037–41
		2007	2042–46	2042–46	2041–44
	Millan	2000	2061–67	2059–64	2055–59
		2015	2068–74	2065–70	2059–63
Blackcomb	Farinotti	2000	2046–51	2046–50	2044–47
		2007	2049–54	2049–53	2046–49
	Millan	2000	2089–2100	2080–87	2071–76
		2015	2096–(>2100)	2085–91	2074–78

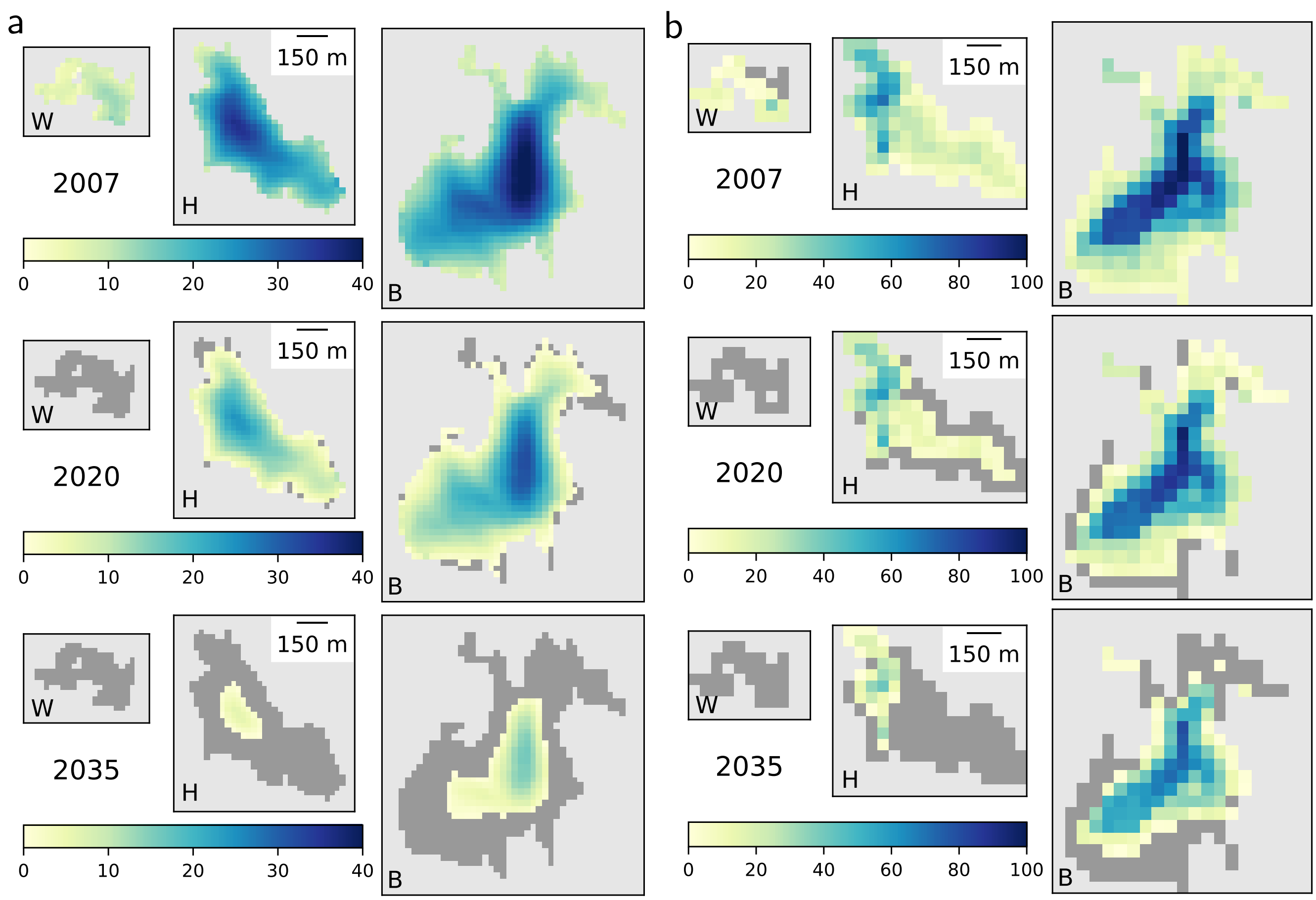

Fig. S10. Spatially distributed projections of ice thicknesses (m) using the mass-balance model initialized in 2000 under CMIP6 SSP2 with an ice density of 850 kg m^{-3}. Distributions shown for 2007, 2020 and 2035 for Whistler (W), Horstman (H) and Blackcomb (B) Glaciers. (a) Farinotti and others (2019) ice-thickness model. (b) Millan and others (2022) ice-thickness model. Note the change in colour scale between (a) and (b).

Table S6. Whistler (W), Horstman (H) and Blackcomb Glacier (B) DDFs, in units of mm w.e. $^\circ$C^{-1} d^{-1}, and disappearance dates for scenarios where the density of snow, annual accumulation, temperature and accumulation lapse rates are varied by $\pm$20% from their reference values (bold). Note that W DDF is the average of H DDF and B DDF. Mass-balance model initialised with the Millan and others (2022) ice thicknesses in 2007 under CMIP6 SSP2.

	W DDF	H DDF	B DDF	Whistler	Horstman	Blackcomb
Density of snow (72.4 kg m^{-3})	1.48	1.43	1.54	2039	2064	2088
Density of snow (90.5 kg m^{-3})	**1.66**	**1.60**	**1.72**	**2038**	**2063**	**2086**
Density of snow (108.6 kg m^{-3})	1.84	1.76	1.91	2037	2063	2084
Annual accumulation (824 cm a^{-1})	N/A	N/A	N/A	2034	2058	2077
Annual accumulation (1030 cm a^{-1})	N/A	N/A	N/A	**2038**	**2063**	**2086**
Annual accumulation (1236 cm a^{-1})	N/A	N/A	N/A	2042	2071	2094
Temp. lapse rate (4.59 °C km^{-1})	1.54	1.47	1.60	2042	2070	2093
Temp. lapse rate (5.74 °C km^{-1})	**1.66**	**1.60**	**1.72**	**2038**	**2063**	**2086**
Temp. lapse rate (6.89 °C km^{-1})	1.80	1.73	1.86	2034	2058	2078
Acc. lapse rate (358 cm a^{-1} km^{-1})	1.63	1.56	1.69	2038	2064	2086
Acc. lapse rate (447 cm a^{-1} km^{-1})	**1.66**	**1.60**	**1.72**	**2038**	**2063**	**2086**
Acc. lapse rate (537 cm a^{-1} km^{-1})	1.69	1.63	1.76	2038	2065	2085

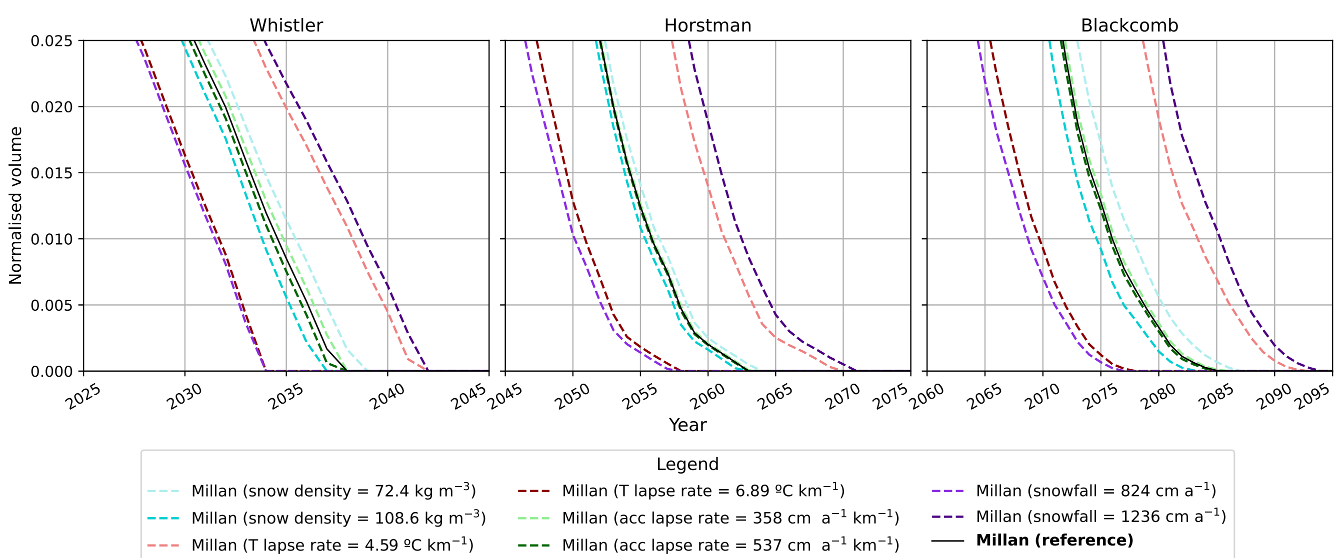

Fig. S11. Normalised glacier volume initialised at 1.0 with the Millan and others (2022) ice-thickness model in 2007 under CMIP6 SSP2 for cases varying the following parameters by $\pm$20% from their reference values: density of snow, annual accumulation, temperature (T) and accumulation (acc) lapse rate.

Table S7. Rates of area change in $km^2\,a^{-1}$ for Whistler, Horstman and Blackcomb Glaciers. Top section: values determined from least-squares linear regression of glacier area as a function of time; these include regressions that are unweighted, weighted inversely proportional to uncertainties (1/err) or the logarithm of uncertainties (1/log(err)), and piecewise pre-2010 and post-2011. Bottom section: values determined from applying the mass-balance model under the CMIP6 SSP2 scenario with an ice density of $850\,kg\,m^{-3}$ to the Farinotti and others (2019) and Millan and others (2022) ice-thickness models variously initialised in 2000, 2007 and 2015.

Glacier	Unweighted regression	Weighted (1/err)	Weighted (1/log(err))	Piecewise: Pre-2010	Post-2011
Whistler	−0.0042	−0.0025	−0.0042	−0.0047	−0.0051
Horstman	−0.0066	−0.0068	−0.0063	−0.0058	−0.0130
Blackcomb	−0.0082	−0.0069	−0.0081	−0.0088	−0.0097
	Farinotti, 2000	Millan, 2000	Farinotti, 2007	Millan, 2015	
Whistler	−0.0042	−0.0027	−0.0046	−0.0032	
Horstman	−0.0075	−0.0055	−0.0084	−0.0063	
Blackcomb	−0.0112	−0.0067	−0.0013	−0.0075	

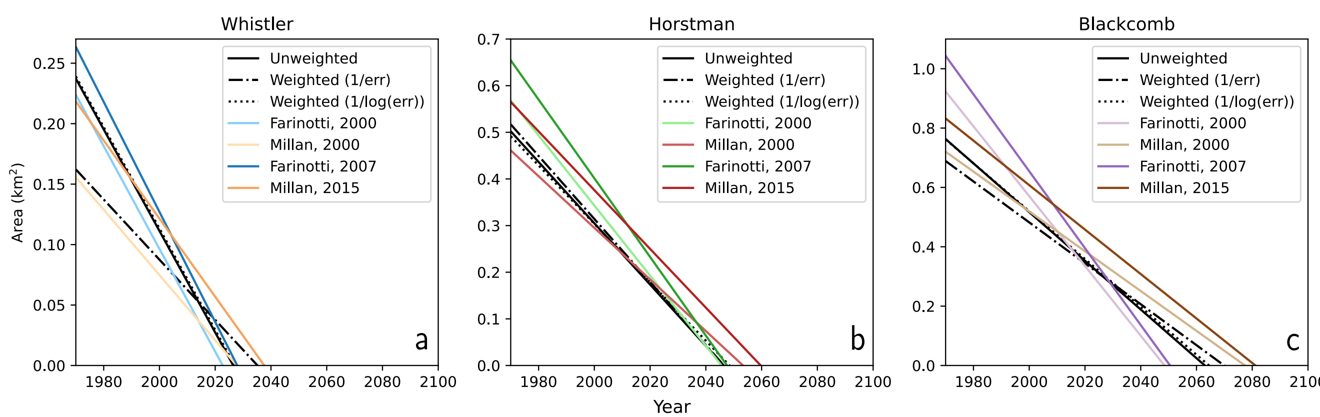

Fig. S12. Glacier area versus time determined using a subset of the methods described in Table S7, with the exception of the piecewise regression (see legend). (a) Whistler Glacier. (b) Horstman Glacier. (c) Blackcomb Glacier.

REFERENCES

Barton M (2017) Twenty-seven years of manual fresh snowfall density measurements on Whistler Mountain, British Columbia. *Atmos. Ocean*, **55**(3), 144–154, ISSN 0705-5900, 1480-9214 (doi: 10.1080/07055900.2017.1331157)

Bevington AR and Menounos B (2022) Accelerated change in the glaciated environments of western Canada revealed through trend analysis of optical satellite imagery. *Remote Sen. Environ.*, **270**, 112862, ISSN 00344257 (doi: 10.1016/j.rse.2021.112862)

Bolch T, Menounos B and Wheate R (2010) Landsat-based inventory of glaciers in western Canada, 1985–2005. *Remote Sens. Environ.*, **114**(1), 127–137, ISSN 00344257 (doi: 10.1016/j.rse.2009.08.015)

European Space Agency (2025) Sentinel-2. https://sentiwiki.copernicus.eu/web/sentinel-2

Farinotti D, Huss M, Fürst JJ, Landmann J, Machguth H, Maussion F and Pandit A (2019) A consensus estimate for the ice thickness distribution of all glaciers on Earth. *Nat. Geosci.*, **12**(3), 168–173, ISSN 1752-0894, 1752-0908 (doi: 10.1038/s41561-019-0300-3)

Government of British Columbia (2025) Digital air photos of B.C. https://www2.gov.bc.ca/gov/content/data/geographic-data-services/digital-imagery/air-photos

Leigh JR, Stokes CR, Carr RJ, Evans IS, Andreassen LM and Evans DJA (2019) Identifying and mapping very small (<0.5 km2) mountain glaciers on coarse to high-resolution imagery. *Journal of Glaciology*, **65**(254), 873–888, ISSN 0022-1430, 1727-5652 (doi: 10.1017/jog.2019.50)

Maussion F, Hock R, Paul F, Raup B, Rastner P, Zemp M, Andreassen L, Barr I, Bolch T, Kochtitzky W, McNabb R and Tielidze L (2023) The Randolph Glacier Inventory version 7.0 User guide (doi: 10.5281/ZENODO.8362857), publisher: Zenodo Version Number: v1.0

Maxar Technologies (2025) WorldView-3. https://resources.maxar.com/data-sheets/worldview-3

Millan R, Mouginot J, Rabatel A and Morlighem M (2022) Ice velocity and thickness of the world's glaciers. *Nat. Geosci.*, **15**(2), 124–129, ISSN 1752-0894, 1752-0908 (doi: 10.1038/s41561-021-00885-z)

Muñoz Sabater J (2019) ERA5-Land hourly data from 1950 to present (doi: 10.24381/CDS.E2161BAC)

Pacific Climate Impacts Consortium (2023) Statistically Downscaled Climate Scenarios (Method: MBCn). Downloaded from https://data.pacificclimate.org/portal/downscaled_gcms/map/ on 23 April 2025

Pacific Climate Impacts Consortium (2025) BC Station Data - Provincial Climate Dataset. Downloaded from https://www.pacificclimate.org/data/bc-station-data on 31 March 2025

PBC PL (2024) Planet Labs: Satellite Imagery & Earth Data Analytics. https://api.planet.com

Pelto MS and Pelto J (2025) The Loss of Ice Worm Glacier, North Cascade Range, Washington USA. *Water*, **17**(3), 432, ISSN 2073-4441 (doi: 10.3390/w17030432)

Planet Developers (2025) PlanetScope. https://docs.planet.com/data/imagery/planetscope/

Resort Municipality of Whistler (2006) Aerial Photo 2006. https://webmap.whistler.ca/html5viewer/index.html?viewer=externalgis/

Whistler Avalanche Forecasters (2025) Seasonal Weather Stats at Pig Alley 1971-2025